npj | digital medicine

Article

Published in partnership with Seoul National University Bundang Hospital

https://doi.org/10.1038/s41746-024-01380-6

Advances in the estimation of body fat percentage using an artificial intelligence 2D-photo method

Tathiany J. Ferreira[1], Igor C. Salvador[1], Carolina R. Pessanha[1], Renata R. M. da Silva[1], Aline D. Pereira[2], Maria A. Horst[3], Denise P. Carvalho[4], Josely C. Koury[5] & Anna P. T. R. Pierucci[1] ✉

There is a growing need to evaluate the agreement between the field methods and integrate artificial intelligence (AI) using two-dimensional (2D) photos for enhanced real-world analysis. This study evaluated the agreement between AI-2D photos and the clinical reference method, dual-energy X-ray absorptiometry (DXA) to estimate the body fat percentage (BFP). Other methods were also investigated, including skinfolds, A-mode ultrasound, and bioelectrical impedance analysis (BIA). This cross-sectional study was conducted on 1273 adults of both sexes. The Bland–Altman plots, Lin's Correlation Coefficient of Agreement (CCC), and error analyses were calculated. AI-2D photos demonstrated substantial agreement with DXA presenting the highest agreement (CCC ≥ 0.96) among all the investigated methods. InBody-270 and Omron HBF-514 BIA devices showed moderate agreement (CCC = 0.90 to 0.95) for all participants, age groups >30 years, and body mass index >25 kg/m^2. AI-2D photos can be interchangeable with DXA, providing a practical, accessible alternative and an easy-to-use system for BFP estimation.

Body composition (BC) refers to the proportion of different compartments of the human body, including fat mass (FM) and fat-free mass (FFM), which comprises muscles, bones, organs, and water[1]. Accurately assessing these components can provide valuable insights into an individual's risk for various health conditions and can be used as a key tool for assessing nutritional status, monitoring clinical interventions, and developing nutritional strategies[1,2].

Methods for assessing BC are based on two-compartment (2C), three-compartment (3C), four-compartment (4C), or multi-compartment models[2]. The simplest is the 2C model, which involves splitting the body into FM and FFM. The 3C model introduces a third compartment, which can be water, allowing for a more accurate estimation of hydration status and muscle mass or bone mineral content, resulting in a breakdown of FM, bone mass, and FFM. The 4C model considered the most precise, further separates the FFM into water, protein, and minerals and also includes total body water. Multi-compartment models require the direct analysis of the major elements of the body[2,3].

Several BC techniques are available for estimating the FM and the body fat percentage (BFP). Among the gold standard methods for analyzing BC are magnetic resonance imaging and dual-energy X-ray absorptiometry (DXA)[1]. DXA is a 3C model and is the reference standard for assessing bone mineral density. Technological improvements have enabled the use of DXA in new applications, offering the possibility of evaluating FM and BFP[4], and has been widely used as a reference method to validate other methods for adults in clinical research[5–8]. However, this procedure is expensive, requires trained personnel, and is limited in accessibility to large-scale population studies. Additionally, exposure to ionizing radiation in DXA, though minimal, raises concerns for frequent assessments[1].

Portable devices, such as bioelectrical impedance analysis (BIA) and fat thickness measurement tools, offer practical alternatives for BC assessment[1–3,9]. BIA is a 3C method that estimates FM, lean mass, and body water or bone mineral content[1]; however, its accuracy is limited by factors such as hydration status and variability across devices, particularly in individuals with extreme BC such as those with obesity and athletes[10]. Subcutaneous fat thickness can be measured using 2C methods, including a plicometer, which assesses skinfold (SF) thickness at various body sites, or A-mode ultrasound (US), which employs sound waves to determine the thickness of subcutaneous fat[3]. SF measurements rely on the evaluator's skill and require physical contact, showing lower accuracy in populations with obesity[11]. A-mode US, while a relatively simple procedure, requires an experienced technician; interpretation remains subjective and challenging, and measurement techniques are not yet fully standardized[9]. Although

[1]Josué de Castro Institute of Nutrition, Federal University of Rio de Janeiro, Rio de Janeiro, RJ, Brazil. [2]Institute of Geography, State University of Rio de Janeiro, Rio de Janeiro, RJ, Brazil. [3]Faculty of Nutrition, Federal University of Goias, Goiania, Goias, Brazil. [4]Carlos Chagas Filho Institute of Biophysics, Federal University of Rio de Janeiro, Rio de Janeiro, RJ, Brazil. [5]Institute of Nutrition, State University of Rio de Janeiro, Rio de Janeiro, RJ, Brazil. ✉e-mail: pierucci@nutricao.ufrj.br

generally less accurate, these methods are well-established and heavily validated[3,9,12–14].

Recently, the use of computer vision and artificial intelligence (AI) with two-dimensional (2D) photos has gained prominence in large-scale BC assessment. This approach can reduce human error and speed up analysis time[15]. This new method uses 2D photos captured with a conventional smartphone camera to estimate the total BFP. AI-2D photo assessment provides an accurate and noninvasive estimate of BFP[16,17]. Studies have reported a high concordance between AI-2D photo and DXA, with only a small variation in the percentage error, compared with other equipment used to estimate BFP. However, further validation across diverse populations is required to confirm this finding[16–18].

Considering the significant diversity and advances in BC assessment methods, investigating the effectiveness of an AI-based method combined with BIA, A-mode US, and SF, compared to the gold standard DXA, is crucial. Thus, this study aimed to evaluate the agreement of multiple portable device methods, including new technology with the use of AI with DXA for assessing BFP in adults. By exploring the accuracy, accessibility, and practicality of these methods, we hypothesize that new technology AI performs higher accuracy than the established field methods as it overcomes most of their limitations and AI-based solutions can serve as excellent alternatives to traditional techniques, potentially revolutionizing BC assessment in clinical and research settings.

Results

Participants

The sample population comprised 1273 individuals, mainly women (54.6%), with a mean age of 35 years, height of 168.29 ± 9.25 cm, weight of 74.25 ± 16.81 kg, body mass index (BMI) of 26.11 ± 5.01 kg/m^2, and BFP of 31.80 ± 9.60 assessed by DXA (Table 1).

Body composition

The AI-2D photo demonstrated substantial agreement (CCC = 0.98) with DXA in all participants, which was higher than that of all the other methods evaluated. The InBody-270 and Omron HBF-514 showed moderate agreement (CCC = 0.92 and 0.91, respectively), while the MaltronBF900, SF (Durnin and Rahaman for men and SF Jackson and Pollock2 3S for women), InBCA F-500, and A-mode US (Durnin and Rahaman for men and SF Jackson and Pollock2 3S for women) showed poor agreement (CCC < 0.90) in the overall participants. The agreement analysis between the methods shows that AI-2D photo, Omron HBF-514, and InBCA F-500 achieved a lower bias percentage of –1.24%, –3.79%, and –7.23%, respectively. In contrast, only AI-2D photo and MaltronBF900 did not show proportion bias ($p = 0.273$ and $p = 0.106$, respectively) among all participants (Table 2).

In a sex-specific evaluation, the AI-2D photo method showed the lowest bias and the best agreement with DXA in men and women, with substantial concordance (CCC = 0.98 for men, CCC = 0.96 for women). Other methods, including MaltronBF900, Omron HBF-514, and InBody-270, showed lower bias but poor agreement with DXA (CCC < 0.90) (Table 2).

Analysis by age group revealed that the AI-2D photo method consistently achieved one of the lowest bias percentages across all age ranges, with the lowest bias in the 30–39 and 40–49 age groups (–1.92% and –0.70%, respectively). Other methods, including the US and SF based on Durnin and Rahaman, Omron HBF-514, and Maltron BF900, also demonstrated low bias percentages across different age groups, particularly in individuals aged 18–29 and 50–65 years. The AI-2D photo method achieved the lowest MAE, MAPE, and MSE values for all age groups and showed substantial agreement compared to DXA (CCC = 0.97–0.98). InBody-270 showed moderate agreement for all ages (CCC = 0.90–0.95), and Omron HBF-514 showed moderate agreement for individuals >30 years old aged 30–39 years, 40–49 years, and 50–65 years (CCC = 0.91–0.92). The other methods showed poor agreement for all age groups (CCC < 0.90) (Supplementary Table 1).

Regarding the BMI range, the AI-2D photo achieved the lowest MAE, MAPE, and MSE values for BMI ranges and showed substantial agreement compared to DXA (CCC = 0.97–0.98). The InBody-270 and Omron HBF-514 analyzers showed moderate agreement for a BMI range of 25–29.9 kg/m^2 (CCC = 0.92) and BMI ≤ 30 kg/m^2 (CCC = 0.95 and 0.93, respectively). The AI-2D photo, US based on Durnin and Rahaman, and the Omron HBF-514 exhibited the lowest bias percentages (–1.64%, 1.85%, and –7.20%, respectively) in individuals with a BMI ≤ 24.9 kg/m^2. For the BMI range of 25–29.9 kg/m^2, the Omron HBF-514, MaltronBF900, and AI-2D photo showed the least bias (–0.83%, –1.03%, and –1.43%, respectively) for. In the category of BMI ≥ 30 kg/m^2, the Omron HBF-514, AI-2D photo, and MaltronBF900 recorded the lowest bias percentages (–0.12%, 0.18%, and –0.70%, respectively) (Supplementary Table 2).

A colored representation of the CCC for all participants stratified by sex, age, and BMI is presented in Fig. 1. The methods with the highest agreement values are depicted in the Bland–Altman plots: AI-2D photo, InBody-270, Omron HBF-514, SF and US Durnin and Rahaman for men and SF and US SF Jackson and Pollock2 3S for women (Fig. 2).

The results from the AVA-030 analysis and the Sloan equations, Eq. 1: SF Jackson and Pollock 3S, and SF Jackson, Pollock, and Ward 4S for SF and A-mode US performed well below expectations and are therefore described in Supplementary Table 3. Error and agreement analyses for all methods by age, sex, and BMI are presented in Supplementary Table 4 and Figs. 1–10.

Discussion

This study investigated the agreement between the BFP predicted by the AI-2D photo and other varied prediction methods (SF equations, A-mode US, and BIA devices) and the BFP by the reference method (DXA) within a sample of healthy adults. The findings demonstrate a high agreement level between AI-2D photo and DXA for sex, age, and BMI classification range compared to the lower agreement of the other methods.

Advances in optical technology have provided methods to evaluate BC using images to estimate BFP in a practical and fast manner and achieve reliable results without the need for a trained professional in anthropometry or radiology[17]. The AI-2D photo showed high precision, concordance, and accuracy when automated machine learning was used to estimate the body FM in eutrophic and overweight adults[8]. Thus, the AI-2D photo method is simple and requires minimal equipment, usually a mobile camera and an AI application. This makes the technique more accessible and easier to implement in environments where more advanced techniques are not available; compared with DXA, the AI-2D photo method is generally more cost-effective.

Our findings support the validity of AI-2D photos in estimating BFP compared with DXA. Majmudar et al. [17] reported similar results, wherein the visual BC estimated by 2D images achieved the lowest BFP error compared with DXA. It also showed greater general concordance with DXA, and lower concordance limits compared to BIA and air displacement plethysmography. Nana et al. [16] estimated BFP with 2D digital images using smartphones and a foot-to-foot BIA device (TANITA BC-313); 2D imaging showed a higher concordance with the DXA data than did the BIA device in adult participants. In the present study, a proportional bias was not observed for the AI-2D photo in the analysis, except for patients with BMI ≥ 30 kg/m^2, which demonstrates that the data presented a homogeneous distribution.

BC estimation by the AI-2D photo could have some advantages, as this method is not influenced by factors such as hydration status, specific equations for the population studied, high-cost equipment, or the need for trained professionals[16–18]. The wide availability of smartphones suggests that the use of photos and suitable applications to evaluate BFP can play a significant role in quantifying adiposity in a more practical, economical, and precise manner[17]. Moreover, AI-2D photos can be widely used, enabling more accurate measurement and monitoring of BFP in individuals of different weight ranges. With its simplicity of use and affordable cost, people can regularly monitor their body fat[17]. Furthermore, BC assessment using AI-2D photos allows remote monitoring. The benefits of remote patient monitoring include the ability to identify potential health issues and changes over time, provide immediate intervention, and reduce the need for in-person visits. With access to healthcare deemed as a significant barrier to

Table 1 | General characteristics, anthropometric measurements, body mass index classification, and body fat percentage for all and according to sex

Variables	All	Men	Women
N (%)	1273 (100)	578 (45.4)	695 (54.6)
Age, Years			
18–29	528 (41.5)	259 (49.1)	269 (50.9)
30–39	345 (27.1)	171 (49.6)	174 (50.4)
40–49	176 (13.8)	67 (38.1)	109 (61.9)
50–65	224 (17.6)	81 (36.2)	143 (63.8)
Weight, kg	74.25 ± 16.81	83.20 ± 15.05	66.81 ± 14.40
Height, cm	168.29 ± 9.25	175.62 ± 6.60	162.19 ± 6.21
BMI, kg/m²			
≤24.9	606 (47.6)	215 (35.5)	391 (64.5)
DXA, BFP	28.27 ± 8.10	20.51 ± 5.46	32.54 ± 5.83
25–29.9	440 (34.6)	247 (56.1)	193 (43.9)
DXA, BFP	32.12 ± 8.97	26.06 ± 6.47	39.87 ± 4.78
≥30	227 (17.8)	116 (51.1)	111 (48.9)
DXA, BFP	40.59 ± 8.66	34.09 ± 6.39	47.39 ± 4.49

Data are described as mean ± standard deviation and percentage.
BFP body fat percentage, *BMI* body mass index, *DXA* dual-energy X-ray absorptiometry.

assessing health conditions, remote applications can provide promising results for measuring and improving health[19].

Although it is a promising method, the AI-2D photo does not currently provide details about the difference between visceral and subcutaneous adipose tissue and total body water or bone mineral content estimate. The AI model was trained on photos of people wearing skimpy, tight clothing. Clothing that covers parts of the body, loose clothing, and images that are too dark or blurry, may result in inaccuracies. Other variables that affect accuracy include extreme camera tilt, excessive distance, or not following the app's recommended position. Furthermore, future research should explore the agreement between BFP estimates obtained using this technique for self-assessment and estimates obtained with the assistance of a trained technician and in non-research environments.

BIA devices are widely used for assessing BC; however, their accuracy and clinical value are often questioned[20]. Our findings show that the AI-2D photo method agrees more with DXA than BIA; only InBody-270 and Omron HBF-514 devices demonstrate moderate concordance with DXA. The BIA devices use different technologies and algorithms to calculate the BC. The equations and mathematical models used to interpret the bioelectrical impedance data may vary, influencing the results[21]. This variation may also reflect the use of an excessively homogeneous reference population by the manufacturer when developing device algorithms, potentially limiting the accuracy and applicability of the results to more diverse populations[13]. Moreover, most manufacturers do not indicate whether the FM results come from a predictive equation or a subtraction calculation, limiting researchers' critical analysis.

Our results revealed a proportion bias in the BIA analysis. Proportional bias refers to the systematic tendency of a measurement method to underestimate or overestimate values relative to a reference standard, depending on the actual value of the measurement. It is an important parameter as it can determine whether people with specific characteristics, such as higher or lower amounts of FM or FFM, can be accurately assessed[22]. Although we observed an underestimation of the BPF using the BIA devices, there was moderate agreement with the DXA based on BMI ranges (25–29.9 and ≥30 kg/m²). Our results are similar to those of Hurt et al.[23], who reported a greater agreement in BMI ranges of 25–29.9 kg/m² (CCC = 0.94) and 30–34.9 kg/m² (CCC = 0.94). Although the variation in the results could potentially be explained by the different algorithms used on each device to calculate the BFP, factors such as the number of electrodes, model, conductivity, and electrode disposition could also contribute to the differences in the results between the devices[10,24].

Multifrequency BIA devices are expected to be more precise than single-frequency ones owing to their ability to penetrate different tissues[25]. However, in our study, the dual-frequency InBody-270 and single-frequency Omron HBF-514 showed higher concordance values and lower concordance limits, MAE, MAPE, and MSE with DXA compared with other multi-frequency and single-frequency methods. These findings suggest that the frequency of the device did not affect the agreement with DXA, but the moderate agreement indicates the need for cautious interpretation.

SF is traditionally the most popular method for assessing BC and is widely used by professionals in various settings, including clinical, sports, and hospital environments[3]. A-mode US can provide a precise assessment of skin thickness, adipose tissue, and muscle at specific sites, with minimal tissue compression. Previous studies have described good agreement between SF and DXA in adult participants[26] and Miclos-Balica et al.[27] showed that A-mode US is highly reliable for BFP estimation (more precise for men than for women); however, the present study found no concordance between the BFP predictive equations in these methods and DXA. This lack of agreement may be attributed to factors such as SF and A-mode US being dependent on the choice of the predictive equation to estimate FFM and, consequently, BFP, which depends on the population, age, measurement quality, and sex of the individual[2]. Additionally, the development and validation of predictive equations in other ethnic groups, and the higher deviation of anthropometric measurements performed on individuals with obesity compared to those performed on individuals of adequate body weight may justify this result[3,28,29].

Analyses of the data regarding the agreement between methods with the raw BFP data usually show an increase in the difference as the BMI increases[12]. In this study, the Bland–Altman plot was analyzed as a percentage of difference, which is preferable for the variability of the proportional difference (constant coefficient of variation), and demonstrated how each method presented more errors relative to DXA. Thus, the differences expressed as percentages of the values were more useful when the variability of the differences increased with the magnitude of the measurement[30]. We analyzed our results as a percentage of the difference and observed that methods that exhibited increased BMI showed no difference in the magnitude of error. These results suggest that evaluating the percentage difference is an additional model for evaluating the differences between BC methods and allowing complementary interpretations.

The limiting factors of the research include measurements that were performed only once (except for anthropometry and AI-2D photo, which were performed in duplicate). However, all assessments were performed during the same session. The strengths of the current study are the large and heterogeneous sample and the analyses being performed by the same anthropometrist. DXA was used as a clinical reference for BC, and the best assessment protocols were adopted.

Our results demonstrated that the AI-2D photo can be interchangeable with DXA; it is a practical and accessible alternative and has an easy-to-use system for BFP estimation. These findings make valuable contributions to the implementation of modern BC analysis methods in clinical practice. The other methods did not provide the same results and showed poor agreement; therefore, the predictive equation, assessor training, calibration, and equipment used must be considered. Evaluating the agreement between BFP estimates using AI-2D photo for self-assessment, in non-research environments, and evaluation of specific populations, such as individuals who perform physical activity at different levels, menopausal women, and those with clinical conditions, is recommended for future studies.

Methods

Study design and participants

This cross-sectional study was conducted at the Laboratory of Development of Foods for Special Needs and Educational Purposes, Health Sciences Center, Federal University of Rio de Janeiro,

Table 2 | Agreement and error analysis among body fat percentages using different methods compared to DXA considering all participants and stratified by sex

Method	*N*	Agreement analysis			Errors analysis		
		CCC	Bias, %	*P*-value*	MAE	MAPE, %	MSE
All							
AI-2D photo	1272	**0.98**	**−1.24**	**0.273**	1.56 ± 1.3	5.01 ± 3.8	4.02 ± 5.9
InBody-270	1273	0.92	−11.69	<0.0001	3.40 ± 2.2	11.93 ± 9.1	16.48 ± 19.5
Omron HBF-514	1268	0.91	−3.79	<0.0001	3.19 ± 2.5	11.38 ± 10.7	16.56 ± 25.8
Maltron BF900	1069	0.82	−8.64	**0.106**	4.56 ± 3.5	15.76 ± 14.2	33.21 ± 50.3
SF[a]	1077	0.79	−12.18	<0.0001	3.79 ± 2.9	12.98 ± 12.3	22.91 ± 32.1
InBCA F-500	1264	0.78	−7.23	<0.0001	4.87 ± 3.5	17.20 ± 16.7	35.63 ± 48.6
A-mode US[a]	1057	0.69	−13.1	<0.0001	3.98 ± 3.2	13.25 ± 16.0	25.88 ± 38.5
Men							
AI-2D photo	578	**0.98**	**−2.03**	**0.359**	1.38 ± 1.1	5.44 ± 4.2	3.20 ± 4.9
InBody-270	578	0.87	−15.13	<0.0001	3.55 ± 2.4	14.94 ± 10.6	18.16 ± 22.0
Omron HBF-514	574	0.83	−7.00	**0.229**	3.44 ± 2.6	14.44 ± 12.3	18.62 ± 25.8
SF[a]	386	0.81	−5.19	0.012	3.73 ± 2.9	14.89 ± 11.3	22.15 ± 31.2
Maltron BF900	481	0.79	−2.87	**0.105**	3.91 ± 3.3	17.44 ± 17.3	26.22 ± 57.9
A-mode US[a]	471	0.78	−3.89	<0.0001	3.94 ± 3.2	16.07 ± 16.5	25.49 ± 38.5
InBCA F-500	461	0.63	−4.64	<0.0001	4.74 ± 3.6	21.03 ± 21.1	35.19 ± 53.8
Women							
AI-2D photo	694	**0.96**	**−0.58**	**0.133**	1.72 ± 1.3	4.66 ± 3.5	4.74 ± 6.5
InBody-270	695	0.89	−8.83	<0.0001	3.24 ± 2.1	9.30 ± 6.7	14.91 ± 17.2
Omron HBF-514	694	0.88	−1.13	**0.127**	2.94 ± 2.4	8.75 ± 8.8	14.44 ± 23.2
Maltron BF900	588	0.73	−13.37	<0.0001	5.30 ± 4.4	14.74 ± 11.8	47.42 ± 127.7
InBCA F-500	692	0.69	−9.36	**0.276**	4.92 ± 3.4	13.90 ± 11.1	35.43 ± 42.6
SF[a]	589	0.68	−17.97	<0.0001	6.05 ± 3.4	16.39 ± 8.8	47.85 ± 48.8
A-mode US[a]	586	0.55	−20.53	<0.0001	7.25 ± 4.4	19.70 ± 11.6	71.73 ± 77.6

Data are expressed as mean ± standard deviation. Bold entries indicate best results for each row.
AI-2D photo artificial intelligence two-dimensional photo, *CCC* concordance correlation coefficient, *MAE* mean absolute error, *MAPE* mean absolute percentage error, *MSE* mean squared error, *SF* Skinfolds *US* Ultrasound.
* *p*-value of the proportional bias of the Bland–Altman linear regression analysis. A statistically significant model coefficient indicates the presence of proportional bias between devices ($p < 0.05$).
[a] The predictive equations by Durnin and Rahaman (for men) and Jackson and Pollock2 3S (for women) were selected for SF and US due to their higher CCC.

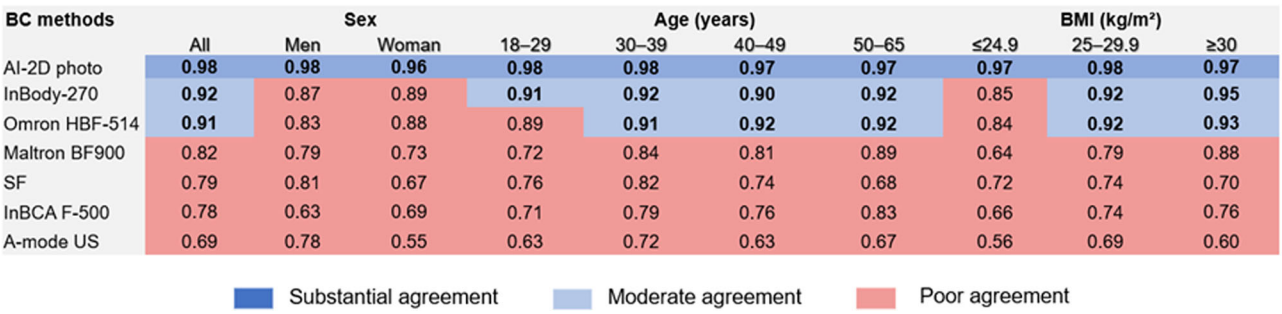

Fig. 1 | Lin's Concordance Correlation Coefficient (CCC) of the various methods evaluated with DXA as the reference for all and stratified for sex, age, and BMI. The colors and cutoff points were adopted: dark blue (0.95-0.99= substantial strength of agreement), light blue (0.90–0.95= moderate strength of agreement), and red (<0.90 poor strength of agreement). AI-2D photo Artificial intelligence two-dimensional photo, BC body composition, BMI body mass index, SF Skinfold, US Ultrasound.

following the Declaration of Helsinki and approved by the ethics committee for research of the Clementino Fraga Filho University Hospital of the Federal University of Rio de Janeiro (protocol number: 5.271.068). Volunteers were recruited through social media platforms (Facebook and Instagram) between September 2021 and February 2022. The study sample comprised individuals of both sexes, aged 18–65 years (Fig. 3).

The inclusion criteria were as follows: weight ≤150 kg due to equipment limitations, no history of amputation, impaired walking, and absence of a pacemaker. The participants were oriented with the pre-exam protocol which included: (1) no consumption of alcohol and caffeine 12 h before the exam; (2) no exercise or going to saunas 8 h before the exam; (3) fasting for 4 h before the exam; (4) bladder emptying before the exam; (5) wearing of bathing clothes, such as swimming trunks for men and sports bra and shorts

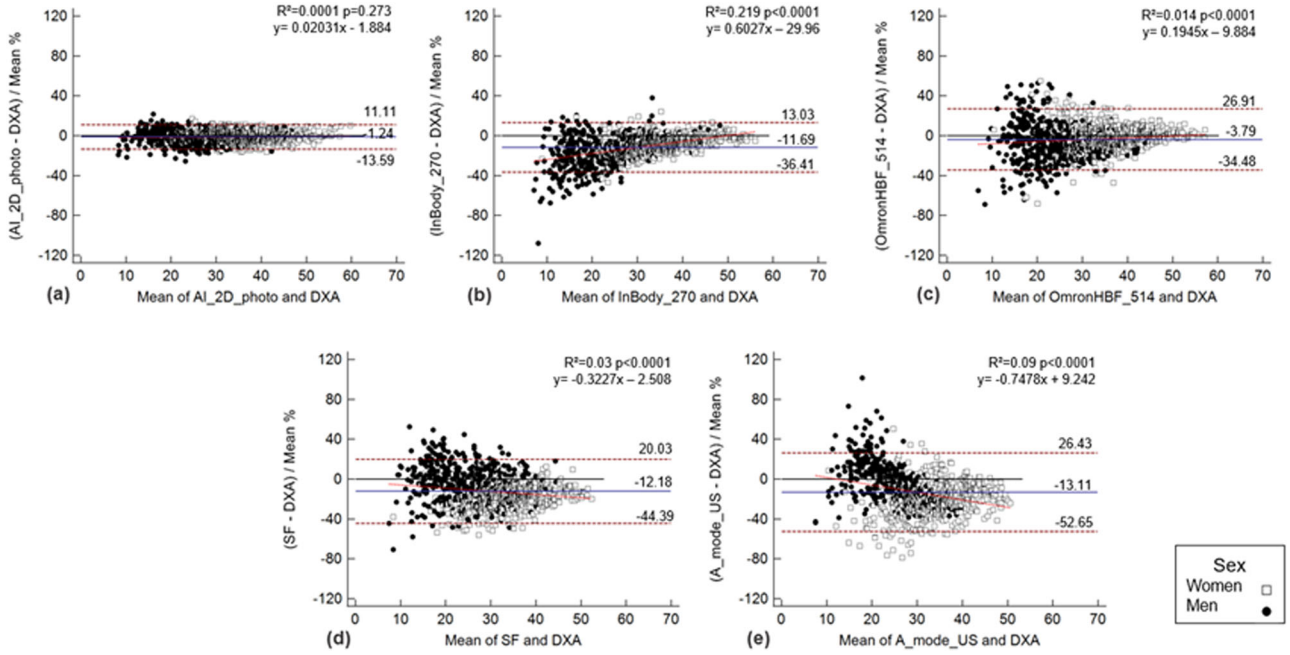

Fig. 2 | Bland–Altman analyses of the percentage of the difference of portable BC devices compared to DXA for the estimation of BFP in all participants. a AI-2D photo, **b** InBody-270, **c** Omron HBF-514, **d** SF: Predictive equations Durnin and Rahaman (for men) and Jackson and Pollock2 3S (for women), and **e**: A-mode US: Predictive equations Durnin and Rahaman (for men) and Jackson and Pollock2 3S (for women). The horizontal blue lines are the mean, the dashed brown is ±1.96 SD and the dashed red lines are the fitted regression lines. White square= women, black circle= men.

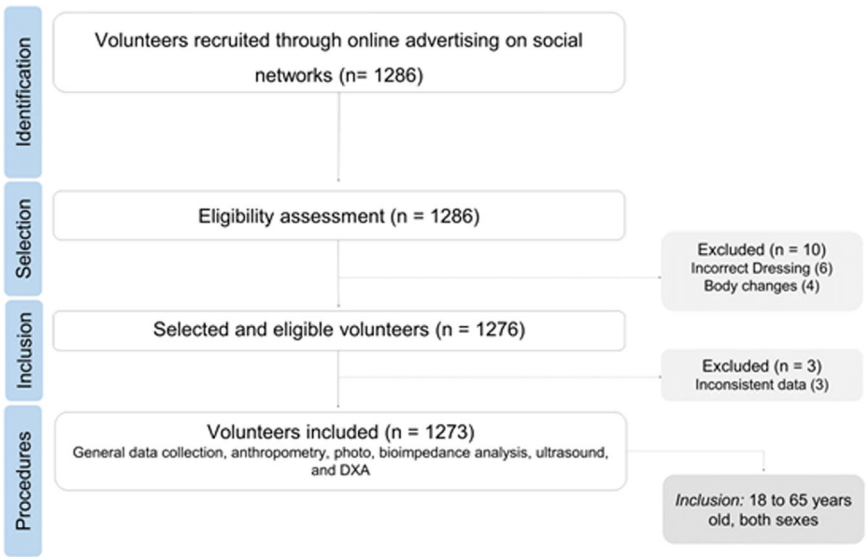

Fig. 3 | Study sampling flowchart according to STROBE. The figure provided represents an overview of the identification, selection, inclusion, and procedures used to determine the number of participants included in the study.

for women, without metal parts; (6) taking off of all metal accessories, such as rings, earring, and piercings; (7) female participants were asked to be present on the day of collection outside their menstrual period. Participants with any tissue alterations (muscular, bone, or fat), edema, movement limitations, menstrual period, pregnancy, refusal to participate at any stage of the study, or failure to follow the protocol were excluded from the study.

General information was obtained using a structured questionnaire that included age, sex, participation in physical exercise (yes or no), and previous diagnosis of diseases (yes or no). The time of last meal intake and physical activity, date of last menstruation, and duration of the menstrual period were assessed to monitor possible external variables. This information was self-reported. All participants voluntarily agreed to participate in the study, and written informed consent was obtained. The authors also affirm that human research participants provided informed consent for the publication of the images in Fig. 4. The volunteers were evaluated using SF, US, BIA, AI-2D photo, and DXA with a 1-min interval between each method.

Anthropometrical measurements

Stature was measured using an Avanutri AVA-305 stadiometer (AvaNutri, Três Rios, Brazil), graded to 0.1 cm. The participants were instructed to stand in front of the stadiometer in an orthostatic position, with their heels united and their heads positioned in the Frankfurt position. Body mass was

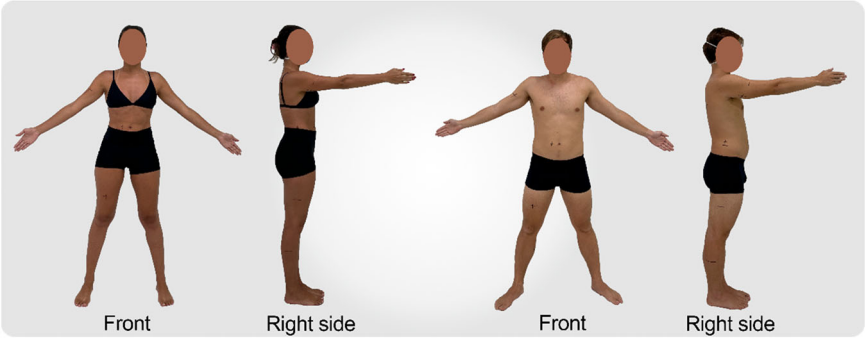

Fig. 4 | Photo protocol, positions, and vestments used in this study. The individuals were instructed to position themselves with legs and arms apart until there were no contact points between them or the torso, respectively. The palms were positioned forward, and the fingers joined. This stance was used for the front-facing photograph. The individual was then instructed to turn to the right side for the camera, with the arm closest to the camera extended, the shoulder in flexion, and the back of the hand facing the camera. The arm and leg on the side farthest from the camera were to remain hidden behind the body.

measured using an InBody-270 (InBody, Seoul, Korea), graded to 0.1 kg. BMI was calculated by dividing the weight (kg) by the square of the height (m)[31].

AI-2D photo

Photographs were analyzed using an AI-based body image assessment application (Shaped, Rio de Janeiro, Brazil). This application utilizes 2D camera images combined with deep learning and a machine learning sex-based approach to estimate BFP. The method involves the following steps: (i) segmentation of the human body; (ii) human pose estimation; (iii) feature extraction and (iv) BFP prediction. The participants were instructed to stand with their legs and arms, ensuring no points of contact between themselves or with their trunk, as described by the manufacturer (Fig. 4). Two photographs (frontal and right profiles) were captured against a white background with the front camera of an iPhone 11 (Apple, Inc.) positioned on a pedestal approximately two meters away from the individuals.

Segmenting the human body in a digital image involves accurately detecting all objects within an image and precisely segmenting each instance. This process involves detecting and localizing the body (as in object detection) and classifying each pixel (as in semantic segmentation) to separate different instances of the same category. For this task, the MS COCO dataset, which includes images of humans with segmentation annotations, is utilized. Then, a trained R-CNN model with a ResNet101 backbone, using the TensorFlow framework, is employed to perform instance segmentation of human bodies[32].

Human pose estimation is the process of identifying and localizing keypoints of the human body in images. The objective is to detect specific parts of the human anatomy, such as joints and facial features, and to determine their spatial configurations. The model architecture adopted was PersonLab[33], which applies a bottom-up approach for human pose estimation and consists of two main stages: keypoint detection and keypoint grouping into individual person instances.

- Keypoint detection (with heatmap generation): The first stage involves detecting all visible keypoints in the image. For each keypoint type K generates a heatmap pk(x) that indicates the probability of a keypoint being present around each pixel x. Valid keypoints can be sorted and selected using these probabilities.
- Keypoint grouping: Once the keypoints are detected and selected, they are associated with individual person instances. This is achieved using mid-range pairwise offsets and recurrent offset refinement.

The next step is featuring extraction, which transforms raw data into a structured format, emphasizing significant patterns to improve the performance and efficiency of machine learning models. The extracted features include 24 Euclidean distances (normalized by image size) based on keypoints detected during human pose estimation, as well as input parameters such as age, weight, and height. Each keypoint represents an image coordinate, that can be defined using $KF_n = (XF_{(n)}, YF_{(n)})$ Eq. (1) for frontal image and $KR_n = (XR_n, YR_n)$ Eq. (2) for right side images.

$$DF_n = \sqrt{(XF_n - XF_{(n+1)})^2 + (YF_n - YF_{(n+1)})^2} \quad (1)$$

$$DR_n = \sqrt{(XR_n - XR_{(n+1)})^2 + (YR_{(n)} - YR_{(n+1)})^2} \quad (2)$$

DF_n represents the Euclidean distance for frontal body image keypoints and DRn represents the Euclidean distance for right body image keypoints. The feature vector to be used as input to perform the BFP prediction is represented as follows:

Attributes = $[Age, Weight, Height, D_{F(1)}, D_{R(1)}, D_{F(2)}, D_{R(2)}, \ldots, D_{F(12)}, D_{R(12)}]$

Regression models are statistical techniques designed to estimate relationships among variables. They are commonly used in data analysis, forecasting, and machine learning to predict continuous outcomes based on one or more predictor variables. Separate models have been developed for each sex: one for predicting BFP in males and another for predicting BFP in females. These models are implemented using the scikit-learn Python library, with hyperparameters optimized through RandomSearch. For each prediction, the sex of the individual is first determined; if male, the prediction is made using the male-specific model, and if female, the female-specific model is used. The general regression model can be represented as follows (Eq. 3):

$$y = \beta_0 + \beta_1 x_1 + \beta_2 x_2 + \ldots + \beta_{27} x_{27} \quad (3)$$

In this equation, 27 attributes (presented in the feature extraction step) are used as input features to predict the BFP (denoted as y).

DXA

BPF was estimated using a DXA GE Prodigy Advance device (GE Healthcare, Madison, Wisconsin, USA) with the enCore 2008 software version 12.20 in automatic full-body scan mode. The participants were placed in the supine (dorsal) position and instructed to remain still throughout the procedure. The examinations were conducted by a single, trained, and qualified professional following the quality control procedures recommended by the manufacturer and the official recommendations of the International Society for Clinical Densitometry[34]. If the participant's a body area was larger than the equipment reading area, the examination was performed on the right side of the body and repeated on the left side[4].

BIA

BFP estimation by BIA was performed using five devices: InBody-270 (InBody, Seoul, Korea), double frequency (20 e 100 kHz) and tetrapolar with eight electrodes; InBCA F-500 (InBCA, Shenzen, China) multifrequency (5, 50, 250, 500 kHz) and tetrapolar with eight electrodes; Omron HBF-514 (Omron, Kioto, Japan), single frequency (50 kHz), and tetrapolar with four electrodes; AVA-030 (AvaNutri Três Rios, Brazil), single frequency (50 kHz), hand-to-hand model with four electrodes; and MaltronBF900

Table 3 | Equations used to estimate body density and fat percentage

Reference (year)	*N*	Points	Validation method	Equation	BFP
Durnin and Rahaman[39]	191	Biceps; Triceps: Subscapular; iliac crest	Underwater weighing	D (g/ml) = 1.1610–0.0632 log (BISF + TRSK + SBSF + SISK)	Siri (1961) BFP = ((4.95/D)–4.50) *100
Sloan[38]	50	Mid-thigh; Subscapular	Underwater weighing	D (g/ml) = 1.1043–0.001327 TSF–0.001310 SSF	Brozek (1963) BFP = 100(4.570/D–4.142)
Jackson et al.[41]	331	Tricpes, abdominal, iliac crest, mid-thigh	Underwater weighing	D = 1.0960950–0.0006952(TRSF + ABSF + SISK + TSF) + 0.0000011(TRSF + ABSF + SISK + TSF)^2–0.0000714 (age in years)	Siri (1961) BFP = ((4.95/D)–4.50) *100
Jackson and Pollock[40] Eq. 1	685	Tricpes, abdominal, iliac crest	Underwater weighing	D = 1.089733 - 0.0009245 (TRSF + ABSF + SISK) + 0.0000025 (TRSF + ABSF + SISK)^2–0.0000979 (age in years)	Siri (1961) BFP = ((4.95/D)–4.50) *100
Jackson and Pollock[40] Eq. 2	685	Triceps, iliac crest, mid-thigh	Underwater weighing	D = 1.099421–0.0009929 (TRSF + TSF + SISK) + 0.0000023 (TRSF + TSF + SISK)^2–0.0001392 (age in years)	Siri (1961) BFP = ((4.95/D)–4.50) *100

BFP body fat percentage, *ABSF* abdominal skinfolds, *BISF* Biceps skinfold, *D* density, *SBSF* subscapular skinfold, *SISF* suprailiac skinfold, *SSF* scapular skinfold, *TRSF* triceps skinfold, *TSF* thigh skinfold.

(Maltron, Essex, England), single frequency (50 kHz) and bipolar with four manual electrodes. The devices do not provide predictive equations for BF calculation.

Fat thickness

Subcutaneous fat thickness was measured at the triceps, subscapular, biceps, iliac crest, abdominal, mid-thigh, and calf sites according to the ISAK protocol[35] with a digital plicometer (Cescorf, Brazil) and a portable A-mode US system, BodyMetrix® BX2000 (IntelaMetrix). Measurements were performed on the right side of the body by a certified ISAK Level 2 anthropometrist. When the difference between measurements was less than 5%, the mean value was used. When a greater difference was observed, a third measurement was performed, and the median value was used.

Equations for body density and body fat percentage

Body density (BD) and BFP were calculated using predictive equations available for the A-Mode US portable device. The Brozek[36] or Siri[37] equation was used to convert BD into BFP. The following predictive equations for BD and BFP were selected for men, respectively: Sloan (1967)[38] and Brozek (1963)[36], Durnin and Rahaman (1967)[39] and Siri (1956)[37]; for women, two equations by Jackson and Pollock (1985)[40] and Siri (1956)[37] were used, described as Eq. 1: SF Jackson and Pollock 3S and Eq. 2: SF Jackson and Pollock2 3S and one equation of Jackson, Pollock, and Ward (1980)[41] and Siri (1956)[37], described as SF Jackson, Pollock, and Ward 4S (Table 3).

Statistical analysis

The sample size calculation was performed using a Bias (%) of –0.67 with a margin of error of 10%, an alpha of 0.05, and a beta of 0.2[17,42]. Thus, the minimum sample size was 720 individuals. The power analysis was conducted using the correlation test statistic for dependent samples, with the post-hoc analysis associated with the alpha, sample size, and power. Accordingly, using an alpha of 0.05 and a sample size of 1273, the test power was 99%. All analyses were performed using G*Power 3.1.9.7 software.

The sample distribution was analyzed using the Shapiro–Wilk test. The descriptive data are expressed as mean ± standard deviation and percentage. Agreement analyses were performed using the Bland–Altman approach to assess the agreement between each method with the DXA. The results are described as differences and plotted differences as percentages. Linear regression was used to evaluate the proportional bias of the SF, BIA, US, and AI-2D photo[43]. The mean absolute error (MAE), mean absolute percentage error (MAPE) and mean square error (MSE) were calculated. Lin's Concordance Correlation Coefficient (CCC) was used to assess the concordance between each method with the DXA[44]. The strength of the agreement criteria for CCC was according to the McBride procedure: CCC < 0.90, poor agreement; CCC: 0.91–0.95, moderate agreement; CCC: 0.96–0.99, substantial agreement; and CCC > 0.99, almost perfect agreement[45]. Analyses were performed for all participants and according to sex (men and women), age (18–29, 30–39, 40–49 and 50–65 years), and BMI (≤24.9, 25–29.9, and ≥30 kg/m^2). Statistical significance was set at $p < 0.05$. Statistical analyses were performed using MedCalc version 20.215.

Data availability

These data are proprietary and will be used for research findings. However, the authors can provide access to the final results upon request to verify our findings.

Code availability

The results were obtained using the software for each method. The authors did not develop any equipment or software used in the study. All data analysis and visualizations were done in MedCalc (version 20.215) using data extracted from the software.

Received: 12 May 2024; Accepted: 10 December 2024;
Published online: 18 January 2025

References

1. Holmes, C. J. & Racette, S. B. The utility of body composition assessment in nutrition and clinical practice: an overview of current methodology. *Nutrients* **13**, 2493 (2021).
2. Kuriyan, R. Body composition techniques. *Indian J. Med. Res.* **148**, 648–658 (2018).
3. Kasper, A. M. et al. Come back skinfolds, all is forgiven: A narrative review of the efficacy of common body composition methods in applied sports practice. *Nutrients* **13**, 1075 (2021).
4. Messina, C. et al. Body composition with dual energy X-ray absorptiometry: from basics to new tools. *Quant. Imaging Med Surg.* **10**, 1687 (2020).
5. Kogure, G. S. et al. Concordance in prediction body fat percentage of Brazilian women in reproductive age between different methods of evaluation of skinfolds thickness. *Arch. Endocrinol. Metab.* **64**, 257–268 (2020).
6. Blue, M. N. M., Tinsley, G. M., Ryan, E. D. & Smith-Ryan, A. E. Validity of body-composition methods across racial and ethnic populations. *Adv. Nutr.* **12**, 1854 (2021).
7. Antonio, J. et al. Comparison of dual-energy X-ray absorptiometry (DXA) versus a multi-frequency bioelectrical impedance (InBody 770) device for body composition assessment after a 4-week hypoenergetic diet. *J. Funct. Morphol. Kinesiol* **4**, 23 (2019).
8. Farina, G. L., Orlandi, C., Lukaski, H. & Nescolarde, L. Digital single-image smartphone assessment of total body fat and abdominal fat using machine learning. *Sensors* **22**, 8365 (2022).
9. Wagner, D. R. Ultrasound as a tool to assess body fat. *J. Obes.* **2013**, 280713 (2013).
10. Kyle, U. G. et al. Bioelectrical impedance analysis-part II: utilization in clinical practice. *Clin. Nutr.* **23**, 1430–1453 (2004).
11. Bacchi, E., Cavedon, V., Zancanaro, C., Moghetti, P. & Milanese, C. Comparison between dual-energy X-ray absorptiometry and skinfold thickness in assessing body fat in overweigh/obese adult patients with type-2 diabetes. *Sci. Rep.* **7**, 1–8 (2017).
12. Achamrah, N. et al. Comparison of body composition assessment by DXA and BIA according to the body mass index: a retrospective study on 3655 measures. *PLoS ONE* **13**, e0200465 (2018).
13. Siedler, M. R. et al. Assessing the reliability and cross-sectional and longitudinal validity of fifteen bioelectrical impedance analysis devices. *Br. J. Nutr.* **130**, 827 (2023).
14. Marra, M. et al. Assessment of body composition in health and disease using bioelectrical impedance analysis (bia) and dual energy x-ray absorptiometry (dxa): a critical overview. *Contrast Media Mol. Imaging* **2019**, 3548284 (2019).
15. Higgins, M. I., Marquardt, J. P., Master, V. A., Fintelmann, F. J. & Psutka, S. P. Machine learning in body composition analysis. *Eur. Urol. Focus* **7**, 713–716 (2021).
16. Nana, A. et al. Agreement of anthropometric and body composition measures predicted from 2D smartphone images and body impedance scales with criterion methods. *Obes. Res Clin. Pr.* **16**, 37–43 (2022).
17. Majmudar, M. D. et al. Smartphone camera based assessment of adiposity: a validation study. *NPJ Digit Med.* **5**, 79 (2022).
18. Sullivan, K. et al. Agreement between a 2-dimensional digital image-based 3-compartment body composition model and dual energy X-ray absorptiometry for the estimation of relative adiposity. *J. Clin. Densitom.* **25**, 244–251 (2022).
19. Starkoff, B. E. & Nickerson, B. S. Emergence of imaging technology beyond the clinical setting: utilization of mobile health tools for at-home testing. *Nutr. Clin. Pract.* **39**, 518–529 (2024).
20. Ward, L. C. Bioelectrical impedance analysis for body composition assessment: reflections on accuracy, clinical utility, and standardisation. *Eur. J. Clin. Nutr.* **73**, 194–199 (2019).
21. Kyle, U. G. et al. Bioelectrical impedance analysis-part I: review of principles and methods. *Clin. Nutr.* **23**, 1226–1243 (2004).
22. McLester, C. N., Nickerson, B. S., Kliszczewicz, B. M. & McLester, J. R. Reliability and agreement of various inbody body composition analyzers as compared to dual-energy X-ray absorptiometry in healthy men and women. *J. Clin. Densitom.* **23**, 443–450 (2020).
23. Hurt, R. T. et al. The comparison of segmental multifrequency bioelectrical impedance analysis and dual-energy X-ray absorptiometry for estimating fat free mass and percentage body fat in an ambulatory population. *J. Parenter. Enter. Nutr.* **45**, 1231–1238 (2021).
24. Campa, F., Toselli, S., Mazzilli, M., Gobbo, L. A. & Coratella, G. Assessment of body composition in athletes: a narrative review of available methods with special reference to quantitative and qualitative bioimpedance analysis. *Nutrients* **13**, 2021 (1620).
25. Abasi, S., Aggas, J. R., Garayar-Leyva, G. G., Walther, B. K. & Guiseppi-Elie, A. Bioelectrical impedance spectroscopy for monitoring mammalian cells and tissues under different frequency domains: a review. *ACS Meas. Sci. Au* **2**, 495 (2022).
26. Golja, P. et al. Direct comparison of (anthropometric) methods for the assessment of body composition. *Ann. Nutr. Metab.* **76**, 183–192 (2020).
27. Miclos-Balica, M. et al. Reliability of body composition assessment using A-mode ultrasound in a heterogeneous sample. *Eur. J. Clin. Nutr.* **75**, 438–445 (2020).
28. Bernhard, A. B., Santo, M. A., Scabim, V. M., Serafim, M. P. & De Cleva, R. Body composition evaluation in severe obesity: a critical review. *Adv. Obes. Weight Manag Control* **4**, 00113 (2016).
29. Hume, P. & Marfell-Jones, M. The importance of accurate site location for skinfold measurement. *J. Sports Sci.* **26**, 1333–1340 (2008).
30. Giavarina, D. Understanding Bland Altman analysis. *Biochem. Med.* **25**, 141 (2015).
31. WHO. *Obesity: Preventing and Managing the Global Epidemic: Report of a WHO Consultation* (World Health Organization, 1998).
32. He, K., Gkioxari, G., Dollár, P. & Girshick, R. Mask R-CNN. *IEEE Trans. Pattern Anal. Mach. Intell.* **42**, 386–397 (2017).
33. Papandreou, G. et al. PersonLab: person pose estimation and instance segmentation with a bottom-up, part-based, geometric embedding model. *Lect. Notes Comput. Sci.* **11218**, 282–299 (2018).
34. Crabtree, N. J. et al. Dual-energy X-ray absorptiometry interpretation and reporting in children and adolescents: the revised 2013 ISCD Pediatric Official Positions. *J. Clin. Densitom.* **17**, 225–242 (2014).
35. Marfell-Jones, M., Olds, T., Stewart, A. & Crater, J. *International Standards for Anthropometric Assessment*. (Potchefstroom, South Africa: International Society for the Advancement of Kinanthropometry - ISAK, 2006).
36. Brožek, J., Grande, F., Anderson, J. T. & Keys, A. Densitometric analysis of body composition: revision of some quantitative assumptions. *Ann. N. Y. Acad. Sci.* **110**, 113–140 (1963).
37. Siri, W. E. Body composition from fluid spaces and density: analyses of methods; in *Techniques for Measuring Body Composition*. *Nutrition* 9 (Washington DC, Natl Acad. Sci. National Res. Council, 1961).
38. Sloan, A. W. Estimation of body fat in young men. *J. Appl. Physiol.* **23**, 311–315 (1967).
39. Durnin, J. V. G. A. & Rahaman, M. M. The assessment of the amount of fat in the human body from measurements of skinfold thickness. *Br. J. Nutr.* **21**, 681–689 (1967).
40. Jackson, A. S. & Pollock, M. L. Practical assessment of body composition. *Phys. Sportsmed.* **13**, 76–90 (1985).
41. Jackson, A., Pollock, M. & Ward, A. Generalized equations for predicting body density of women. *Med Sci. Sports Exerc.* **12**, 175–182 (1980).
42. Pinto, V. F. Estudos clínicos de não-inferioridade: fundamentos e controvérsias. *J. Vasc. Bras.* **9**, 145–151 (2010).
43. Bland, J. M. & Altman, D. G. Measuring agreement in method comparison studies. *Stat. Methods Med. Res.* **8**, 135–160 (1999).

44. Lin, L. I. A concordance correlation coefficient to evaluate reproducibility. *Biometrics* **45**, 255–268 (1989).
45. McBride, G. B. *A Proposal for Strength-of-Agreement Criteria for Lin's Concordance Correlation Coefficient*. National Institute of Water and Atmospheric Research (NIWA) Client Report MOH05201. (New Zealand, 2005).

Acknowledgements

The authors thank all the volunteers who participated in the research. This work was supported by the Foundation Carlos Chagas Filho Research Support of the State of Rio de Janeiro (FAPERJ) process number: E-26/201.042/2021 and SEI260003/001172/2020; and by the Financial Agency of Studies and Projects (FINEP) process number: 0.1.18.0107.00 (PROINFRA).

Author contributions

T.J.F.: Conceptualization. Methodology. Validation. Formal analysis. Research. Writing – original draft. Writing – revision and editing. Visualization. I.C.S.: Conceptualization. Methodology. Validation. Research. Writing – original draft. Writing – revision and editing. Visualization. C.R.P.: Conceptualization. Statistical analysis. Research. Writing – original draft. Writing – revision and editing. Visualization. A.D.P.: Validation. Formal analysis. Writing – proofreading and editing. R.R.M.S.: Research. Writing – original draft. Writing – revision and editing. Visualization. M.A.H.: Writing – original draft. Writing – revision and editing. Visualization. J.C.K.: Writing – revision and editing. Visualization. D.P.C.: Writing – revision and editing, Visualization, and Acquisition of funding. A.P.T.R.P.: Conceptualization. Methodology. Research. Writing – original draft. Writing – revision and editing. Supervision. Project administration. Acquisition of funding.

Competing interests

The authors declare no competing interests.

Additional information

Supplementary information The online version contains supplementary material available at https://doi.org/10.1038/s41746-024-01380-6.

Correspondence and requests for materials should be addressed to Anna P. T. R. Pierucci.